Modelling of the rotating disk electrode in Ionic liquids: difference between water based and ionic liquids electrolytes

A. Giaccherini[1], A. Lavacchi[2]
[1]INSTM, Firenze, Italy, [2]ICCOM - CNR, Firenze, Italy
*Corresponding author: via Lastruccia 3-13 50019, Sesto Fiorentino (FI), andrea.giaccherini@unifi.it

Abstract: The last few years experienced a rapid growth in the application of Ionic Liquids (IL's) to electrodeposition. ILs offer a variety of advantages over aqueous electrolytes. In general ILs show large chemical and thermal stability, high ionic conductivity and an electrochemical window much larger than water. These properties together with their negligible vapor pressure enabling their use at different temperatures without any risk of generating harmful vapors and joined to the absence of hydrogen discharge interfering with electrodeposition processes, as they are essentially hydrophobic, make them the best candidates to be used for the obtainment of homogeneous electrodeposited thin films. This study focuses on the silver electrodeposition from a silver tetrafluoroborate solution in 1-butyl-3-methyltetrafluoroborate BMImBF4. We notice that practical deposition rate at even concentrations were much lower in ionic liquids as compared to water electrolytes an investigation of mass transport has been undertaken. Hydrodynamic voltammetry with Rotating Disk Electrode (RDE) of ferrocene/ferrocinium solutions in BMImBF4 have been performed in order to estimate diffusion coefficient for the different systems. Eventually, simulation of the RDE voltammetry based on the FEA (Finite Elements Analysis) have been performed. Laminar flow has been imposed to compute the steady state solution of the Navier-Stokes equation (laminar flow) and then it has been solved the electrochemical process in the high conductivity regime. Thus solving only the transport proprieties neglecting the potential drop of the electrolyte. Two different process has been simulated: the actual voltammetries in IL and an equivalent voltammetries in water. The former allows to validate the model by means of comparison with the experimental voltammograms, the last allows to rationalize the peculiar mass transport properties of the Ils. In particular, thanks to the comparison of the concentration profiles and fluxes at the steady and quasi-steady states of the potential scan for both systems, we clarified the nature of the unexpected peaks show by the experimental voltammograms.

Keywords: Levich equation, Ionic Liquids, Transport proprieties, RDE, electroanalytical, CFD.

1. Introduction

Research on electrodeposition has recently focused on the quest for new electrolytes alternative to water. This was mainly driven by the need to develop new and green electrodeposition processes. Major breakthroughs were the discovery of Ionic Liquids which application to electrodeposition boomed in the first 2000's and deep eutectic solvents based on environmentally benign compounds (e.g choline and urea). The deposition of an extremely large variety of thin and thick films of metals and alloys from these novel electrolytes has been demonstrated at the lab scale.
The problem related to water-based galvanic bath are, among others, the limited electrochemical window (1.23V) imparing the deposition of many elements (eg. Aluminum, Silicon and Titanium etc…) and involving, in most cases, noxious or polluting chemical species. Oppositely, ionic liquids and DES have stability windows that in certain cases exceed 6V. Despite such definite advatange and the research effort,

IL's are still not fully exploited in the electrodeposition technologies, with only a few systems commercially available solutions for extremely specialized niches of application.
The cause for such slow development of this field is that extremely complex task constituted by the switching electrodeposition from water to IL's. Among several concerns such as the higher costs, stability of the solvents, necessity of dedicated galvanic lines (usually under controlled atmosphere) the transport proprieties affect definitely the stability of the coating process. We focus on this critical aspects of the electrochemical process. A significant difference in viscosity between water electrolytes and IL's exists. Water has a dynamic viscosity of 1 cp while most IL's range between one and two order of magnitude higher than that. By means of FEA (Finite Elements Analysis), as implemented in Comsol Multiphysics, we investigated the mass transport in highly viscous solvents to highlight the differences between electrodeposition in water and that in ionic liquids. Such complexity arises from the fact that viscosity affect both the diffusion coefficient of reacting species and the development of the velocity field in the electrolyte. Thus, things gets more difficult when convection is involved. In this work we report the results of an extensive investigation on convection in a highly viscous Ionic Liquid to unravel the elements that concur to the mass transport limitation of such electrolytes.
To do so we analyze the case the RDE voltammetries performed on the Ferrocene/Ferrocinium redox couple in $BMImBF_4$. This IL is known to have a viscosity of 100 cp that is ideal to emphasize the effect of viscosity on electrodeposition. We have realized a series of experiment in well-defined convective conditions (RDE experiments). These experiments have then be modeled by a finite element analysis to understand the concentration profile and to estimate the size of the boundary layers. The calculation have been performed both in water and in $BMImBF_4$ to highlight the differences between the two solvents.

2. Model

The necessity to understand the nature of the peak present in the RDE voltammetries performed in IL lead to definition of a numerical model of the RDE. The 3D geometry of the RDE has a cylindrical symmetry, thus the numerical domain can be reduced to a simple 2D axisymmetric geometry, constituted by an embedded disk electrode, located on the axis of symmetry of the system (Figure 1). For the purpose of perform a dedicated comparison with experimental data we designed a domain with the same volume and geometry of the real volume interested in the experiments (just the electrolyte under the level of the working electrode). The electrochemical media are constituted by Ferrocene (3.83 mol m^{-3}) in $BMImBF_4$ or water, characterized by chemical and physical proprieties reported in Table 1. The electrochemical reaction controlling the current in the RDE voltammetry is associated with the Ferrocene (FeCen)/Ferrocinium (FeCin) redox couple:

$$FeCen \longrightarrow FeCin + e^-$$

The calculation has been performed by means of the simulation program COMSOL Multiphysics® with the electroanalytical and the CFD (Computational Fluidynamics) modules.

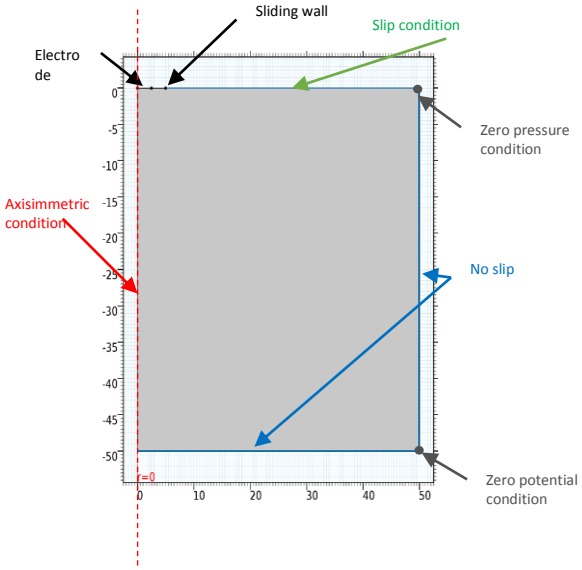

Figure 1. Scheme showing the cell geometry considered for the RDE with the set of boundary condition considered in this work. The electrolyte domain is a square with an edge of 50mm and the segments represent the radius of the embedded disk electrode (1.5mm) and the embedding cylinder (5mm).

2.1 Governing equations

The uncoupled problem has been solved in two step:

1. Solution for the stationary state of the Navier-Stokes equation(1). In a typical «Rotating Disk Electrode» (RDE), the cylindrical symmetry implies a laminar flow even at high rotation speed. Exploiting the symmetry of the system, we reduce the 3D RDE domain to a 2D axisymmetric domain as reported in figure 1. The 3D velocity is reproduced from the 2D velocity field thanks to the use of the "swirl flow" option in COMSOL Multiphysics® which solves implicitlty for the azimuthal coordinate for an axisymmetric problem.

$$k\nabla^2 v - \rho(v\,\nabla v) - \nabla\rho = 0 \qquad \nabla \cdot v = 0 \tag{1}$$

2. The resulting laminar flow advection field has been given as input of the electroanalytical interface, to solve for the time dependent current in order to estimate the characteristic curve of the RDE voltammetry. Usually at the lab-scale, with such very high conducting electrolytes, the distribution of the electric potential can be neglected. In this context the Ohm's law, equation (2) is not considered, while the Nersnt-Plank equation (3) constitute the only governing equation for this part of the model.

$$\nabla^2 \phi_l = -\frac{Q_l}{\sigma_l} \tag{2}$$

$$\underline{N_i} = -D_i \nabla c_i - z_i u_{m,i} F c_i \nabla \phi_l + \underline{u} c_i \tag{3}$$

ϕ_l is the electric potential in the electrolyte; σ_l is the conductivity of the electrolyte and Q_l is the electric charge. In the Nernst-Plank: Where c_i, D_i, u_i, and z_i are the concentration, the diffusion coefficient, the mobility and the charge of the of the i_{th} species, respectively; F the Faraday's constant; $\underline{u}$ the velocity field; R_i the reaction term for A and B. Due to the neglecting of equation (2), meaning that an homogenous distribution of the electric potential in the intermediate assumed, thus
the migration term in equation (3) has been not considered since. In order to calculate the change in composition of the electrolyte near the electrodes due to electron transfer, it's well established the validity of the following Faraday equation (3):

$$R_{i,m} = \frac{-\nu_{i,m} i_{loc,m}}{n_m F} \tag{3}$$

$i_{loc,m}$ is the faradaic current density for the m_{th} process, n_m is the number of electrons exchanged.

2.2 Boundary conditions

Boundary conditions for the Nernst-Plank (3) can be defined as follow (7-9):

$$\underline{i_l} \cdot \underline{n} = i_{total} \quad (7)$$

$$i_{total} = \sum_i i_{loc,m} + i_{dl} \quad (8)$$

$$i_{loc} = i_0 \left(\frac{C_R}{C_R^0} e^{\frac{\alpha_a F \eta}{RT}} - \frac{C_O}{C_O^0} e^{\frac{-\alpha_c F \eta}{RT}} \right) \quad (9)$$

where, $\underline{i_l}$ is the current distribution vector; i_{dl} is the capacitive current density; $i_{loc,m}$ is the faradaic current density for the m_{th} process; i_0 is the exchange current; C_R/C_R^0 is the ratio of the concentration to the bulk concentration; α_a is the electron transfer coefficient; R is the perfect gasses constant; T is the temperature and η is the electrode overpotential defined by equation (10).

$$\eta = \phi_l + \phi_s - E_{eq} \quad (10)$$

Here, $\phi_l + \phi_s$ is the electrical potential drop across the electrode interface.

2.3 Mesh

A dedicated approach to define the correct mesh for the Navier-Stokes equations and the Nernst-Plank equation has been followed. The convergence of the meshes has been tested plotting the algebraic residual of the module of the velocity and of the concentration, respectively for Navier-Stokes and Nernst-Planck equations. Independtly, a cross check of the effect of the mesh convergence was performed, checking the effect of the mesh size on the limiting velocity (Navier-Stokes) and on the limiting current (Nernst-Planck). For Navier-Stokes equations we chose a triangular mesh with the boundary layers on two of the edges, constituted by 50 quadrangular elements, a exponent of 1.05 and the thickness adjustment ratio of 1. The resulting algebraic residual is homogenously under 10^{-12}. For Nernst-Planck we chose a quadrangular mapped mesh with the boundary layers on one edge, constituted by 150 quadrangular elements, a exponent of 1.1 and the thickness of the first layer is adjustment ratio of 1nm. The resulting algebraic residual is homogenously under 10^{-8}.

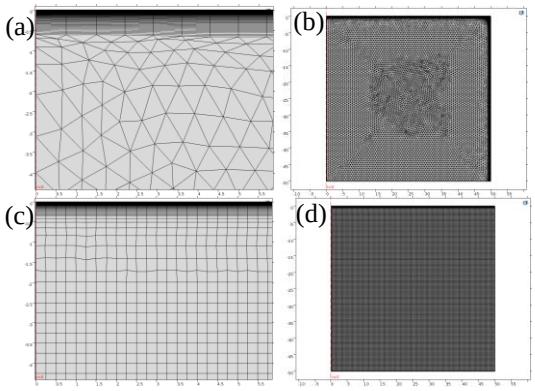

Figure 2. (a) close up (b) overall of the mesh for the Navier-Stokes. (c) close up (d) overall of the Nernst-Planck.

2.4 Chemical and physical proprieties of the electrolytes

	IL	Water
D(FeCen)	1.3 10^{-11} m^2s^{-1} [1]	1.3 10^{-9} m^2s^{-1} [1]
D(FeCin)	1.3 10^{-11} m^2s^{-1} [1]	1.3 10^{-9} m^2s^{-1} [1]
C_0(FeCen)	3.83 mol m^{-3}	3.83 mol m^{-3}
C_0(FeCin)	0 mol m^{-3}	0 mol m^{-3}
i_0	N/D	N/D
η	132 mPa s	0.894 mPa s

Table 1: Physical and chemical constant for the modelling of FeCen in $BMImBF_4$.

Where D are the diffusion coefficient, C_0 the bulk concentration of the electrolyte, i_0 the exchange current density and η the dynamic

viscosity of the IL. The exchange current density has been obtained as the solution of an inverse problem performed by means of comparison with the experimental curve in IL.

3. Results

3.1 Validation

The model has been validated by means of comparison with the experimental data, the comparison between the experimental and theoretical voltammetric curves at 2000rpm and different scan rate ($10mVs^{-1}$, $50mVs^{-1}$ and $100mVs^{-1}$) are depicted in Figure 3. We achieved a very good agreement at the steady state. The agreement at the peak have been achieved by sweeping the exchange current density.

The best agreement is achieved in every case with $1.8\ 10^{-1}$ A m^{-2}.

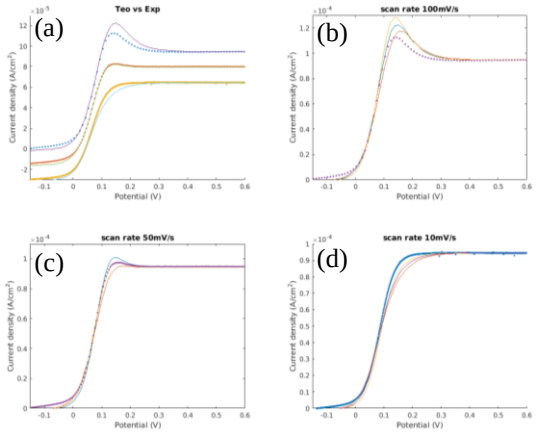

Figure 3. (a) close up (b) overall of the mesh for the Navier-Stokes. (c) close up (d) overall of the Nernst-Planck.

On the other hand using the Levich's law (11) to calculate the diffusion coefficient we obtain $1.6\ 10^{-11} m^2\ s^{-1}$ in contrast with the value obtained by Eisele with chronoamperometric and voltammetric measurements. [1,2]

$$i_L = \beta n F D_0^{2/3} \omega^{1/2} \nu^{-1/6} C_0 \qquad (11)$$

Where i_L is the average current density on the electrode at the steady state, β a constant related to the measure units, n number of electrons involved in the reaction, F the Faraday constant, D_0 the diffusion coefficient of the limiting species, ω the rotation rate, ν kinematic viscosity and C_0 the bulk concentration of the limiting species. Moreover, if we use $1.6\ 10^{-11} m^2\ s^{-1}$ a discrepancy, in the range of few percents, between the numerical and experimental data arises as expected. The cause for the peaks and for the discrepancies in the limiting current will be discussed in the following paragraphs.

3.2 Convection layers

The convection layers can be extrapolated by means of a graphical method from the concentration profiles, as depicted by blue lines in figure 4a,b. We report the concentration profiles for $10mVs^{-1}$, $50mVs^{-1}$ and $100mVs^{-1}$ at the steady state (0.6V) and the peak (0.12V). The three concentration profiles in figure 4a reported for the steady state in IL, are exactly superimposable. While the three concentration profiles for the peak in IL, are not superimposable and the higher the scan rate the higher the discrepancy with the steady state concentration profiles. In water all the six concentration profile (steady state and the peak) are perfectly matching each other. Figure 4c,d report the concentration as function of the distance from the electrodes and the potentials for IL (Figure 4c) and water (Figure 4d). The low potential side of the plot reports the concentration profiles for the kinetic controlled potential range. On the other hand, the high potential side report the mass transport controlled potential range, meaning that the black boxes highlight the transition potential ranges. Remarkably, the transition part of the voltammetry is not affected by the scan rate in water electrolyte, while in IL is scan rate dependent. Higher

the scan rate more extended the transition part is. Moreover, it is worth to notice that the transition part of the voltammetric scan for the 10 mVs^{-1} in IL resembles the transition part for water.

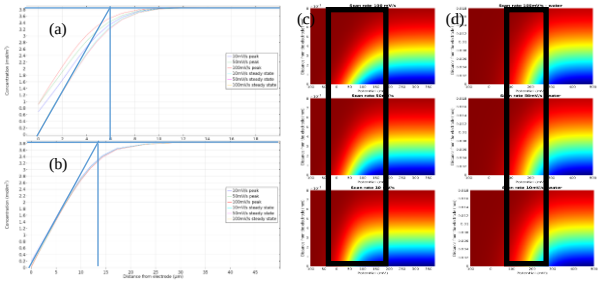

Figure 4. Concentration profiles in IL (a) and in water (b). Concentration as function of the distance from the electrodes and the potentials for IL (c) and water (d).

3.3 Velocity field

The velocity field for an embedded disk in an infinite domain has been analytically described by Von Karman. A popular solution to this problem has been proposed by Cochran. The solution has been used by Levich, obtaining the famous Levich's equation. The assumption that the Cochran solution holds, is necessary for the validity of the Levich's equation. Meaning that the velocity should be perpendicular to the electrode (left hand side of figure 5a,b) very closely to the upper boundary. The velocity field for water seems to be matching the Cochran's solution. A more precise picture is depicted in figure 5c,d, where the profile of the non-dimensional velocity field components calculated in this work are reported. The limiting velocity for water along the axis (V_z) is roughly 0.88, consistent with Cochran's solution (0.8847). For IL the limiting velocity component along z is remarkably lower. In general the non-dimensional velocity field components for water are perfectly matching the Cochran's solution, while for IL substantial difference can be reported. Thus for water the velocity field can be considered developed, in the sense of Cochran solution. On the contrary, for IL the velocity field is not completely developed. Hence, it is not consistent with Levich's equation. [2,3]

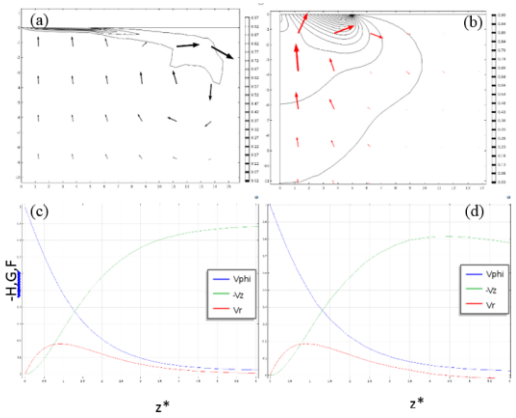

Figure 5. Velocity field near the electrode for water (a) and IL (b). Non dimensional velocity field components for water (c) and IL (d).

4. Conclusion

In this work we report a numerical model of a RDE voltammetry in a finite size domain allowed to understand two unexpected experimental results. Particularly, the peak at 0.12V is unexpected for RDE voltammetries at any practical rotating speed and scan rate. Moreover, the discrepancy of the diffusion coefficient obtained from the experimental rotating speed, with respect to the one calculated by Eisele by means of chronoamperometric and voltammetric measurements. In paragraph 3.1, is shown the very good agreement that we achieved at the limiting current and at the unexpected peak for the RDE voltammtries at 2000rpm and different scan rate ($10mVs^{-1}$, $50mVs^{-1}$ and $100mVs^{-1}$). Given that the exchange current density have been obtained by means of the comparison of the experimental data and several simulation carried at different exchange current density, in particular on

the kinetic controlled potential range. We successfully described the concentration profile, proving that at the peak the concentration profile is not completely developed, while in water it is matching perfectly the concentration profile at the steady state. Moreover, when the peak is not present (at $10mVs^{-1}$) the transition part of the voltammetric scan, depicted in figure 4c, is very similar to the one in water (Figure 4d). Eventually, we found that in this conditions the velocity field for IL (Figure 5b,d) is not well developed, in the sense of Cochran, while for water it is. Likely, this breaks the assumption that must hold to be able to rely on the Levich's equation validity in ionic liquid. We think that the velocity field cannot be well developed in IL since the dragged layer (1.6mm in this condition) is comparable with the radius of embedding cylinder, while for water is ten times smaller. Thus, new geometry should be study in order to be able to reliably apply Levich's equation in IL.

5. References

1. S. Eisele, M. Schwarz, B. Speiser, C. Tittel, Diffusion coefficient of ferrocene in 1-butyl-3-methylimidazolium tetrafluoroborate - concentration dependence and solvent purity, *Electrochim. Acta*. **51** (2006) 5304–5306.

2. Bard, Allen J.; Larry R. Faulkner, Electrochemical Methods: Fundamentals and Applications, 339, Wiley(2000)

3. Y. V. Pleskov, V. Y. Filinovski, *The rotating disc electrode*. Consultants Bureau, Studies in soviet science (1976)